

56. Water Exchange on Hexaaquavanadium(III): a Variable-Temperature and Variable-Pressure ^{17}O -NMR Study at 1.4 and 4.7 Tesla¹⁾²⁾

by Alain D. Hugi, Lothar Helm, and André E. Merbach*

Institut de chimie minérale et analytique de l'Université de Lausanne, 3, place du Château, CH-1005 Lausanne

(20.XII.84)

Water exchange on hexaaquavanadium(III) has been studied as a function of temperature (255 to 413 K) and pressure (up to 250 MPa, at several temperatures) by ^{17}O -NMR spectroscopy at 8.13 and 27.11 MHz. The samples contained V^{3+} (0.30–1.53 m), H^+ (0.19–2.25 m) and ^{17}O -enriched (10–20%) H_2O . The trifluoromethanesulfonate was used as counter-ion, and, contrary to the previously used chloride or bromide, CF_3SO_3^- is shown to be non-coordinating. The following exchange parameters were obtained: $k_{\text{ex}}^{298} = (5.0 \pm 0.3) \cdot 10^2 \text{ s}^{-1}$, $\Delta H^* = (49.4 \pm 0.8) \text{ kJ mol}^{-1}$, $\Delta S^* = -(28 \pm 2) \text{ JK}^{-1} \text{ mol}^{-1}$, $\Delta V^* = -(8.9 \pm 0.4) \text{ cm}^3 \text{ mol}^{-1}$ and $\Delta\beta^* = -(1.1 \pm 0.3) \cdot 10^{-2} \text{ cm}^3 \text{ mol}^{-1} \text{ MPa}^{-1}$. They are in accord with an associative interchange mechanism, I_a . These results for H_2O exchange are discussed together with the available data for complex formation reactions on hexaaquavanadium(III). A semi-quantitative analysis of the bound H_2O linewidth led to an estimation of the proportions of the different contributions to the relaxation mechanism in the coordinated site: the dipole-dipole interaction hardly contributes to the relaxation (less than 7%); the quadrupolar relaxation, and the scalar coupling mechanism are nearly equally efficient at low temperature ($\sim 273 \text{ K}$), but the latter becomes more important at higher temperature (75–85% contribution at 360 K).

Introduction. – Variable-pressure measurements have proven to be an excellent tool to investigate the activation mode of substitution reactions [2]. In the particular case of solvent exchange, where no charge creation or neutralisation occurs during the reaction process, the observed volume of activation directly reflects the modifications of inter-nuclear distances and bond angles from the reactants to the transition state: a dissociative process leads to an expanded transition state, and thus a positive volume of activation, while a negative volume of activation implies a contraction at the transition state, that is an associative activation mode.

High-pressure NMR technique has been used to investigate solvent-exchange reactions on divalent high-spin first-row hexasolvated transition metal ions, and the results show a gradual changeover in substitution mechanism along the series: the early members show I_a behaviour and the latter ones I_d behaviour, the change in activation mode occurring after the d^5 configuration [3]. High-spin trivalent ions have received less attention until now, the only volumes of activation for H_2O exchange known to date being for hexaaquachromium(III) [4] [5] and hexaaquairon(III) [6].

Kinetic studies on ligand-substitution reactions with the hexaaquavanadium(III) ion are scarce, and although it is well-accepted that substitution on this cation proceeds associatively, experimental arguments lay essentially on the comparison of some complex formation rate constants, and on a rather old variable temperature study of H_2O ex-

¹⁾ Part 24 of the series 'High-Pressure NMR Kinetics'. Part 23: [1].

²⁾ These results are part of the Ph.D. thesis of A. H., University of Lausanne, 1984.

change [7]. This latter was performed in presence of Cl^- and Br^- , and we found [8] that these ions form complexes with V^{3+} that obscure the kinetic analysis of the data. We, therefore, decided to reinvestigate the H_2O exchange on $\text{V}(\text{III})$ as a function of temperature, and then to determine the volume of activation of that reaction by variable-pressure measurements. As the widely used perchlorate anion oxidizes the cation too rapidly to be used, we chose as counter-ion the redox inert and non-complexing trifluoromethanesulfonate ion.

Experimental. – *Chemicals and Solutions.* Vanadium trifluoromethanesulfonate, $\text{V}(\text{CF}_3\text{SO}_3)_3$, was prepared by mixing 3.09 g VCl_3 (*Fluka, purum*) with 9.75 g of previously degassed $\text{CF}_3\text{SO}_3\text{H}$ (*Fluka, purum*; hereafter called triflic acid), in an O_2 -free glove box. *Ca.* 5 g of degassed H_2O was vacuum-distilled onto that mixture and then, after homogenization of the soln., distilled off together with HCl formed by the reaction. A fresh portion of *ca.* 2 g of H_2O was distilled onto the mixture, to eliminate the remaining HCl . Finally, the pale green salt was dried by heating to 346 K under vacuum ($8 \cdot 10^{-4}$ Torr). Anal. calc. for $\text{V}(\text{CF}_3\text{SO}_3)_3$ (498.15): V 10.23, F 34.32, C 7.23, S 19.31, Cl 0.00; found: V 9.95, F 33.90, C 6.86, S 18.75, Cl 0.52. This corresponds to the formula: $\text{V}(\text{CF}_3\text{SO}_3)_{2.92}\text{Cl}_{0.08}$.

The compositions of the seven solns. used for the NMR experiments are given in *Table 1*. They were prepared in the glove box by mixing weighted quantities of the vanadium salt and of a previously degassed triflic-acid soln.; the latter was made at the desired concentration by mixing the proper amount of pure triflic acid with ^{17}O -enriched H_2O (*Yeda, Israel, ca.* 10% or 20%, normalized in ^1H).

Table 1. *Composition of Solutions*

Solutions ^{a)}	$\text{V}(\text{CF}_3\text{SO}_3)_3/m$	$\text{CF}_3\text{SO}_3\text{H}/m$	P_m
1 ^{b)c)}	0.303	2.25	0.0342
2 ^{b)}	0.999	2.03	0.1129
3 ^{b)c)d)}	1.526	2.06	0.1725
4 ^{b)c)}	0.301	0.193	0.0341
5 ^{b)c)}	1.468	0.193	0.1665
6 ^{d)}	1.405	1.93	0.1582
7 ^{e)}	0.301	1.97	0.0333

^{a)} All solutions contained *ca.* 20 atom-% ^{17}O , except soln. 7, with *ca.* 10 atom-%.

^{b)} Variable-temperature experiments at 8.13 MHz.

^{c)} Variable-temperature experiments at 27.11 MHz.

^{d)} Variable-pressure experiments at 8.13 MHz.

^{e)} Variable-pressure experiments at 27.11 MHz.

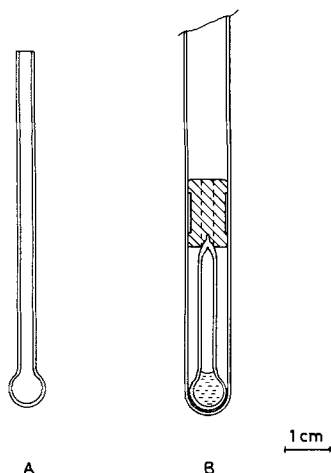


Fig. 1. A) Variable-temperature sample tube before sealing; B) sealed sample tube fitted in a 10-mm o.d. NMR tube

Samples for variable-temperature measurements were introduced into a glass tube (Fig. 1, A) and heat-sealed; the spherical end fits into a 10 mm o.d. NMR tube (Wilmad), and the sealed end is held in place with a PTFE spacer (Fig. 1, B); note that the soln. fills only the spherical part of the tube. Use of spherical samples allows work with small amounts of enriched H₂O and minimizes magnetic field distortion [9]. For the variable-pressure experiments, the samples were introduced into a glass capillary fitted with a PTFE cap, as previously described [10] [11].

Instrumentation. The ¹⁷O-NMR spectra were recorded using a Bruker WP-60 spectrometer equipped with a 1.4 T electromagnet working at 8.13 MHz, and a Bruker CXP-200 instrument with a 4.7 T wide-bore cryomagnet working at 27.11 MHz. For ambient-pressure work, the temp. of the 10-mm NMR tubes was held constant within ± 0.3 K by use of a Bruker BVT-1000 unit and was measured by a substitution technique, using a Pt resistor [12]. Variable-pressure measurements on the WP-60 spectrometer were performed up to 250 MPa with a high-pressure probe similar to that described for ¹³C [13], but adapted for ¹⁷O. Measurements on the CXP-200 spectrometer were performed up to 200 MPa with the high-pressure probe already described [11].

Results and Data Treatment. – Variable Temperature. Typical ¹⁷O-NMR spectra of a vanadium solution at low temperature are shown in Fig. 2; the large signal comes from ¹⁷O nuclei in the bulk H₂O while the upfield-shifted small signal is due to ¹⁷O nuclei of the molecules bound to the paramagnetic ions. The corresponding experimental conditions are given in the caption.

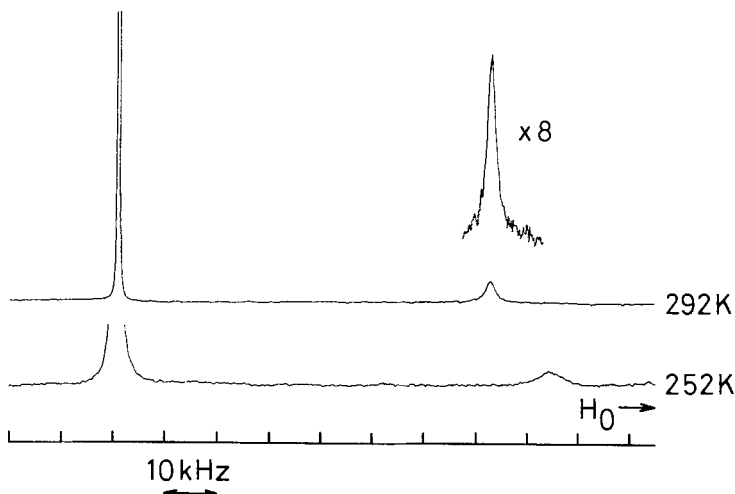


Fig. 2. 27.11-MHz ¹⁷O-NMR spectra of solution 3 (cf. Table 1) showing bulk and bound H₂O at two different temperatures. The upper (lower) spectrum is the result of 77 000 (100 000) scans using a repetition rate of 20 msec and a pulse width of 5 μsec (90° pulse = 50 μsec) in the quadratic detection mode; 2 K data points were used over a total spectral width of 200 kHz.

The expression for the effect of solvent exchange on the transverse relaxation rate, obtained from the free or coalesced water signal in a dilute paramagnetic solution, was first given by Swift and Connick [14], and has been modified to include the outer sphere contribution [11]:

$$\frac{1}{T_{2r}} = \frac{1}{P_m} \left(\frac{1}{T_2} - \frac{1}{T_{2A}^0} \right) = \frac{1}{\tau_m} \left[\frac{T_{2m}^{-2} + (T_{2m} \tau_m)^{-1} + \Delta\omega_m^2}{(T_{2m}^{-1} + \tau_m^{-1})^2 + \Delta\omega_m^2} \right] + \frac{1}{T_{2os}} \quad (1)$$

P_m is the mole fraction of coordinated H₂O, calculated assuming a coordination number of 6 [15], $1/T_2$ is the observed relaxation rate, $1/T_{2A}^0$ is the relaxation rate of the solvent in

absence of paramagnetic ion (measured on a H₂O sample containing only triflic acid at the appropriate concentration), τ_m is the residence time of a coordinated H₂O ligand, T_{2m} is the relaxation time of coordinated H₂O in absence of exchange, $\Delta\omega_m$ is the chemical shift between free and coordinated H₂O in absence of exchange and $1/T_{2os}$ is the outer-sphere relaxation rate.

The residence time τ_m is related to the pseudo-first-order exchange rate constant, k , and to the temperature by the *Eyring* equation:

$$k = \frac{1}{\tau_m} = \frac{k_B T}{h} \exp\left(\frac{\Delta S^*}{R} - \frac{\Delta H^*}{RT}\right) \quad (2)$$

where ΔS^* and ΔH^* are the entropy and the enthalpy of activation for the exchange reaction. The temperature dependence of $\Delta\omega_m$ may be described empirically as a power series of $1/T$ [11], of which only the first two terms will be considered, *i.e.*

$$\Delta\omega_m = \frac{B_1}{T} + \frac{B_2}{T^2} \quad (3)$$

with B_1 equal to the constant part of the *Bloembergen* eqn. [16]:

$$B_1 = -\frac{\omega S(S+1)\gamma_e A}{3\gamma_n k_B} \quad (4)$$

In this equation, ω is the *Larmor* frequency of the observed nucleus, S is the spin quantum number of the paramagnetic ion, γ_e and γ_n are the magnetogyric ratios of the electron and the nucleus, and A is the scalar coupling constant between the electron spin and the nucleus spin.

The outer-sphere relaxation time is assumed to have a simple *Arrhenius* behaviour [17]:

$$1/T_{2os} = A_{os} \exp(E_{os}/RT) \quad (5)$$

Relaxation of a ¹⁷O-nucleus in the first coordination sphere of a V³⁺ ion may be caused by three mechanisms: *i*) an electric quadrupolar relaxation, *ii*) a scalar coupling between the nuclear spin and the electronic spin of the paramagnetic ion, and *iii*) a dipole-dipole interaction with the paramagnetic ion. Thus:

$$1/T_{2m} = 1/T_{2Q} + 1/T_{2S} + 1/T_{2D} \quad (6)$$

Under extreme narrowing conditions, the quadrupolar transverse relaxation rate obeys the following equation [18]:

$$\frac{1}{T_{2Q}} = \frac{3\pi^2}{10} \frac{2I+3}{I^2(2I-1)} \chi^2 \left(1 + \frac{1}{3}\eta^2\right) \tau_c \quad (7)$$

where I is the nuclear spin quantum number, χ is the quadrupolar coupling constant, η is an asymmetry parameter and τ_c is a correlation time for the reorientation of the hexaaqua ion, and obeys an *Arrhenius* behaviour [19].

$$\tau_c = \tau_c^{298} \exp\left(\frac{E_Q}{R} \left(\frac{1}{T} - \frac{1}{298.15}\right)\right) \quad (8)$$

The relaxation *via* scalar coupling of the spins occurs at a rate given by [18]:

$$\frac{1}{T_{2S}} = \frac{1}{3} \left(\frac{A}{\hbar} \right)^2 S(S+1) \left(\tau_{ei} + \frac{\tau_{e2}}{1 + (\omega_1 - \omega_e)^2 \tau_{e2}^2} \right) \quad (9)$$

where A and S have been defined above, τ_{ei} and τ_{e2} are correlation times for this relaxation mechanism, and ω_1 and ω_e are the Larmor frequencies of the nucleus and the electron, respectively. The correlation times depend on the electronic relaxation rates and the water exchange rate:

$$1/\tau_{ei} = 1/T_{ie} + 1/\tau_m \quad (i = 1, 2) \quad (10)$$

Finally, the dipole-dipole interaction allows a relaxation expressed by [18]:

$$\frac{1}{T_{2D}} = \left(\frac{\mu_0}{4\pi} \right)^2 \cdot \frac{\gamma_1^2 \gamma_e^2 \hbar^2 S(S+1)}{15 r^6} \left(4\tau_{d1} + \frac{3\tau_{d1}}{1 + \omega_1^2 \tau_{d1}^2} + \frac{\tau_{d2}}{1 + (\omega_1 - \omega_e)^2 \tau_{d2}^2} + \frac{6\tau_{d2}}{1 + \omega_e^2 \tau_{d2}^2} + \frac{6\tau_{d2}}{1 + (\omega_1 + \omega_e)^2 \tau_{d2}^2} \right) \quad (11)$$

where μ_0 is the permeability constant, r is the V-O distance (taken as the sum of the ionic radii of O^{2-} and V^{3+} : 200 pm [20]), and τ_{d1} and τ_{d2} are correlation times defined by:

Table 2. Relaxation Rates, $1/T_2$, of the Bulk H_2O in Presence of $V(CF_3SO_3)_3$ as a Function of Temperature (for the composition of the solutions, see Table 1)

Solution 1		Solution 2		Solution 3		Solutions 4, 5 resp.	
$10^3/T$ [K ⁻¹]	$1/T_2$ [s ⁻¹]	$10^3/T$ [K ⁻¹]	$1/T_2$ [s ⁻¹]	$10^3/T$ [K ⁻¹]	$1/T_2$ [s ⁻¹]	$10^3/T$ [K ⁻¹]	$1/T_2$ [s ⁻¹]
2.433	1800 ^{a)}	2.526	4714 ^{a)}	2.433	8251 ^{a)}	2.473	1792 ^{a)}
2.458	2286	2.606	5650	2.669	5664	2.604	1424
2.526	1802	2.617	4760	2.784	3464	2.924	305.0
2.606	1392	2.669	4025	2.830	2348	3.106	173.2
2.617	1542	2.759	2165	2.932	1380	3.312	177.4
2.669	1084	2.830	1487	3.009	910.5		
2.784	686.9	2.920	842.3	3.117	582.1	2.536	2800 ^{b)}
2.830	492.8	3.009	577.7	3.214	472.6	2.667	1512
2.932	304.9	3.109	397.6	3.328	432.4	2.799	648.8
3.009	230.7	3.214	341.1	3.410	502.0		
3.117	191.9	3.326	328.9	3.485	571.6		
3.214	190.9	3.410	382.2	3.579	728.3	2.473	11275 ^{a)}
3.328	214.7	3.485	445.5	3.661	967.8	2.604	7967
3.410	255.1	3.579	564.5	3.794	1294	2.924	1317
3.485	299.0	3.661	719.2	3.919	1908	3.106	580.7
3.579	372.1	3.794	966.1			3.312	403.6
3.661	472.2	3.919	1468	2.420	21530 ^{b)}		
3.794	663.7			2.485	17519	2.667	7019 ^{b)}
3.919	954.9			2.530	14614	2.799	3105
				2.595	11142		
2.420	4206 ^{b)}			2.621	8602		
2.485	3462			2.665	6526		
2.530	2735			2.777	3324		
2.595	2160						
2.621	1683						
2.665	1286						
2.777	664.9						

^{a)} At 8.133 MHz. ^{b)} At 27.11 MHz.

$$1/\tau_{d_i} = 1/\tau_{c_i} + 1/\tau_c \quad (i = 1, 2) \quad (12)$$

From this equation, $\tau_{d_1} \leq \tau_c$ and thus, under extreme narrowing condition, $\omega_1^2 \cdot \tau_{d_1}^2 \ll 1$. Furthermore, $\omega_c \gg \omega_1$, so that Eqn. 11 can be simplified as follows:

$$\frac{1}{T_{2D}} = \left(\frac{\mu_o}{4\pi}\right)^2 \cdot \frac{\gamma_i^2 \gamma_e^2 \hbar^2 S(S+1)}{15r^6} \left(7\tau_{d_1} + \frac{13\tau_{d_2}}{1 + \omega_e^2 \cdot \tau_{d_2}^2}\right) \quad (13)$$

The bulk water relaxation rates of five samples with various concentrations in triflic acid (0.19–2.25 *m*) and in vanadium triflate (0.30–1.53 *m*) (see Table 1) were measured between 255 K and 415 K at two different frequencies; the experimental data are given in Table 2. The bound water relaxation rates and the $\Delta\omega_m$'s were only measured for the most concentrated solution, and these data are listed in Table 3. No effect of the acid concentration, nor of the metal ion concentration is apparent (Fig. 3). In the accessible tempera-

Table 3. Chemical Shifts, $\Delta\omega_m$, and Bound H₂O Relaxation Rates, $1/T_{2c}$, in Concentrated $V(CF_3SO_3)_3$ Solution as a Function of Temperature (Solution 3 in Table 1)

$10^3/T [K^{-1}]$	$-\Delta\omega_m \cdot 10^{-5} [s^{-1}]$	$1/T_{2c} [s^{-1}]$	$10^3/T [K^{-1}]$	$-\Delta\omega_m \cdot 10^{-5} [s^{-1}]$	$1/T_{2c} [s^{-1}]$
2.885	(3.7434) ^{a)}	12649	3.315	4.3638	6110
2.951	3.8414	8627	3.429	4.5228	6638
3.044	3.9766	6648	3.550	4.7040	7161
3.115	4.0812	6717	3.677	4.8771	9205
3.137	4.1089	6732	3.819	5.0500	13033
3.238	4.2541	5117	3.964	5.2684	16602

a) This chemical shift is subject to a chemical-exchange contribution, and was, therefore, not used in the numerical analysis (Eqn. 3).

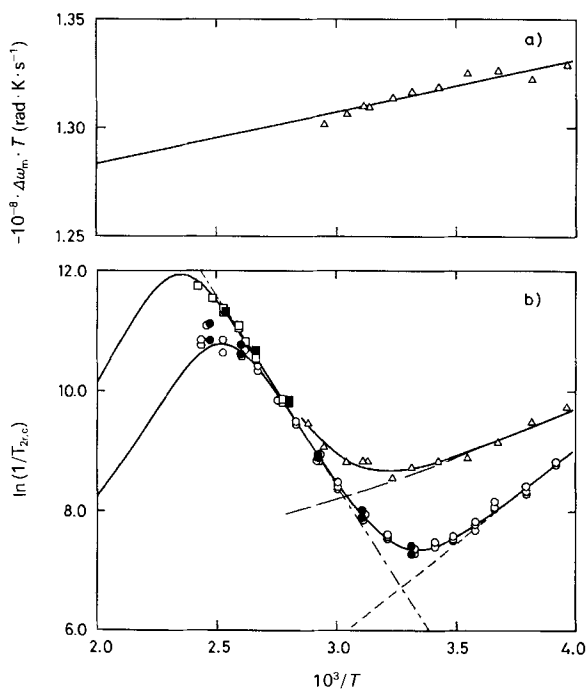


Fig. 3. Chemical shifts (a) and relaxation rates (b) of $V(CF_3SO_3)_3$ solutions as a function of temperature. \circ and \bullet : $1/T_{2r}$ at 8.13 MHz; \square and \blacksquare : $1/T_{2r}$ at 27.11 MHz (filled symbols represent solutions of lower acidity, 4 and 5 in Table 1). \triangle : $\Delta\omega_m \cdot T$ and $1/T_{2c}$ of solution 3. Interrupted lines show contributions of $1/T_{2os}$ (---), $1/\tau_m$ (-.-) and $1/T_{2m}$ (---) to fitted curves (—).

ture range, the $\ln 1/T_{2r}$ curve barely reaches the coalescence point (maximum of the curve), and the so-called 'fast exchange' region [14] is not observable. This allows us, as a first approximation, to neglect the $1/T_{2m}$ term in Eqn. 1, leading to the simplified following equation:

$$\frac{1}{T_{2r}} = \frac{1}{T_{2os}} + \frac{1}{\tau_m} \left(\frac{\Delta\omega_m^2}{\tau_m^{-2} + \Delta\omega_m^2} \right) \quad (14)$$

Thus, the $1/T_{2r}$ and $\Delta\omega_m$ data were analysed with Eqns. 2–5 and 14 by means of a multiset non-linear least-squares computer program, and with six adjustable parameters: ΔH^* , ΔS^* (or k^{298}), A, B_2 , A_{os} and E_{os} . The fitted parameters are given in the first column of Table 4, and the corresponding calculated curves are plotted on Fig. 3. Note that the chemical shift results are plotted as $\Delta\omega_m \cdot T$ against $1/T$, to show the necessity of a quadratic term in Eqn. 3.

Table 4. Kinetic and NMR Parameters Obtained from the Variable-Temperature Study of Aqueous $V(CF_3SO_3)_3$ Solutions. The detailed fitting procedures are described in the text.^{a)}

Fitting Procedure	$1/T_{2m} = 0$	$1/T_{2Q} - Ga^{3+}$		$1/T_{2Q} - Al^{3+}$	
		$T_{1e} = T_{2c}$	$T_{1e} \gg T_{2c}$	$T_{1e} = T_{2c}$	$T_{1e} \gg T_{2c}$
k^{298} [s^{-1}]	495 ± 29	488 ± 28	491 ± 28	487 ± 28	490 ± 28
ΔH^* [$kJ mol^{-1}$]	49.37 ± 0.79	49.62 ± 0.76	49.52 ± 0.76	49.65 ± 0.76	49.55 ± 0.76
ΔS^* [$JK^{-1} mol^{-1}$]	-27.75 ± 2.18	-27.02 ± 2.10	-27.31 ± 2.10	-26.95 ± 2.10	-27.23 ± 2.10
$10^2 \cdot A_{os}$ [s^{-1}]	2.2 ± 1.1	2.4 ± 1.1	2.3 ± 1.1	2.4 ± 1.2	2.3 ± 1.1
E_{os} [$kJ mol^{-1}$]	26.7 ± 1.2	26.6 ± 1.1	26.6 ± 1.1	26.6 ± 1.1	26.6 ± 1.1
A/h [MHz]	4.897 ± 0.044	4.896 ± 0.042	4.896 ± 0.042	4.895 ± 0.042	4.896 ± 0.042
$10^9 \cdot B_2$ [$rad K^{-2}$] ^{b)}	2.38 ± 0.33	2.40 ± 0.31	2.39 ± 0.31	2.40 ± 0.31	2.39 ± 0.31
T_c^{298} [ps]	–	6.0 ± 0.4	6.3 ± 0.4	6.6 ± 0.4	6.9 ± 0.4
E_c [$kJ mol^{-1}$]	–	9.3 ± 2.0	8.7 ± 1.8	7.2 ± 2.7	6.6 ± 2.4

^{a)} Reported errors are standard deviations. ^{b)} At 4.67 T.

Since $1/T_{2m}$ can be neglected in the analysis of $1/T_{2r}$, the relative importance of the different relaxation mechanisms of the ^{17}O nucleus in the bound site can only be obtained from the line-width of the bound- H_2O signal, using the following equation:

$$\frac{1}{T_{2c}} = \frac{1}{\tau_m} + \frac{1}{T_{2m}} \quad (15)$$

This equation is valid as long as $1/T_{2c}$ is much smaller than $\Delta\omega_m$.

The Eqns. 6–13, which define the different contributions to $1/T_{2m}$, can be simplified as follows: the product $\chi(1 + \eta^2/3)^{1/2}$ (Eqn. 7) is taken the same as for pure H_2O , that is 7.58 MHz [21], assuming that coordination does not affect this term. The exchange rate, $1/\tau_m$, is smaller than $10^4 s^{-1}$ in the temperature range where $1/T_{2c}$ is measurable (see Fig. 3), while the electronic relaxation rate of V_{aq}^{3+} have been calculated from 1H -NMR data to be of the order of $5 \cdot 10^{10} s^{-1}$ at 220 K [7]. Thus $1/\tau_m$ can be omitted in Eqn. 10 (and implicitly in Eqn. 12).

The available data do not allow an independent determination of the temperature dependence of each of the remaining parameters, τ_c , T_{1e} and T_{2c} , and some reasonable approximations are needed. The quadrupolar relaxation is an electric phenomenon and,

under extreme narrowing conditions, is independent of the magnetic environment of the nucleus, that is it will not depend on whether the neighbouring metallic ion is diamagnetic or paramagnetic. Besides, the isotropic tumbling time is related to the radius, r , of the species by the *Debye-Stokes-Einstein* equation [18].

$$\tau_c = \frac{4\pi r^3}{3k_B T} \cdot \eta \quad (16)$$

where η is the viscosity of the solution. We will assume that the isotropic tumbling time of a H₂O molecule bound to a V³⁺ ion ($r = 64$ pm) may be approximated by that of a H₂O molecule bound to an Al³⁺ ion ($r = 53$ pm) or, still better, to a Ga³⁺ ion ($r = 62$ pm). We, therefore, used the results of a ¹⁷O-NMR study of H₂O exchange in Al³⁺ and Ga³⁺ solutions of similar ionic strength, *i.e.* similar viscosity, to estimate τ_c [22]. Aqueous solutions of diamagnetic ions are very suitable for the determination of tumbling times since, in the absence of exchange, the relaxation mechanism of ¹⁷O nuclei is purely quadrupolar.

The electronic relaxation times, T_{1e} and T_{2e} , are not known for the V³⁺ ion; in such a situation, two limiting cases can be envisaged, $T_{1e} = T_{2e}$ and $T_{1e} \gg T_{2e}$. It is easily shown that both cases lead to simplified forms of *Eqns. 9* and *13*, characterized by only one electronic relaxation time, T_e , which obeys an *Arrhenius* behaviour:

$$T_e = T_e^{298} \cdot \exp\left[\frac{E_e}{R}(1/T - 1/298.15)\right] \quad (17)$$

Now the $1/T_{2e}$ data can be fitted together with the chemical shift and the bulk H₂O relaxation data, using the whole set of equations and adjusting eight parameters (T_e^{298} , E_e plus the six ones cited above). The parameters of the isotropic tumbling time were set to the values calculated either from the Ga(H₂O)₆³⁺ results ($\tau_c^{298} = 2.54 \cdot 10^{-11}$ s⁻¹, $E_Q = 23.5$ kJ mol⁻¹) or from the Al(H₂O)₆³⁺ results ($\tau_c^{298} = 4.22 \cdot 10^{-11}$ s⁻¹, $E_Q = 20.75$ kJ mol⁻¹) [22]; in both cases, the computer programme used either one or the other limiting conditions about T_{1e} and T_{2e} . This led to four sets of results, displayed in *Table 4*; the excellent agreement of these with the set obtained previously confirm the validity of the assumption $1/T_{2m} = 0$ when analysing the $1/T_{2r}$ and $\Delta\omega_m$ data alone.

One can notice that both limiting cases for the electronic relaxation times lead to quite close values for T_e^{298} and E_e ; this is because, at that high magnetic field, the electron *Larmor* frequency, ω_e , is large enough to make the products $\omega_e^2 \tau_{e2}^2$ (*Eqn. 9*) and $\omega_e^2 \tau_{d2}^2$ (*Eqn. 13*) greater than 1; thus, even if T_{2e} is considered equal to T_{1e} , the second term in brackets is smaller than the first one in these equations.

Fig. 4 shows the percentage of each mechanism contributing to the bound H₂O relaxation rate, in the temperature domain where the coordinated signal is observable; the broad lines correspond to the Ga³⁺ model and the fine lines to the Al³⁺ model. Since the values of τ_c^{298} and E_Q are noticeably different in both models, the lines are not very close, nevertheless, the fitted values of the parameters of T_e are satisfactorily consistent within the two models; this estimation has of course only a semi-quantitative value, due to the many approximations that were made, but general trends can be discerned from *Fig. 4*: first, the dipole-dipole interaction hardly contributes to bound ¹⁷O-nuclei relaxation (because their magnetogyric ratio is small, as compared to that of protons, *e.g.*).

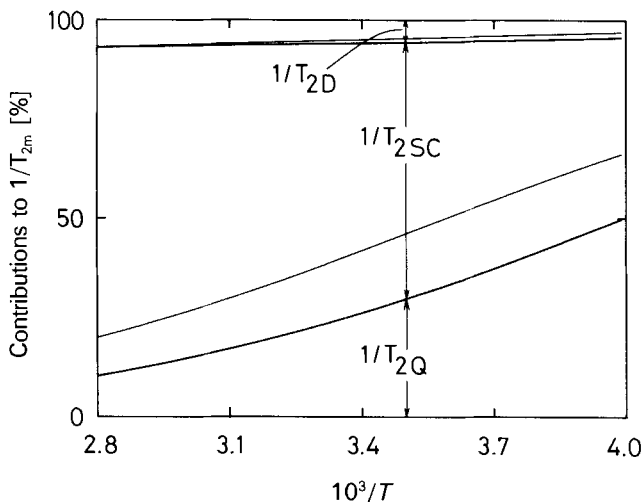


Fig. 4. Estimated contributions of the non-kinetic relaxation mechanisms of ^{17}O nuclei of bound H_2O molecules as a function of temperature, using quadrupolar relaxation data of $\text{Ga}(\text{H}_2\text{O})_6^{3+}$ (—) and $\text{Al}(\text{H}_2\text{O})_6^{3+}$ (—) from [22]

Second, the quadrupolar relaxation and the scalar coupling mechanism are nearly equally efficient at low temperature, but due to the difference in the activation energies between these two mechanisms, the scalar coupling mechanism becomes more important at higher temperature. However, even at 350 K, the contribution of the quadrupolar relaxation remains significant.

Variable Pressure. According to transition state theory, the volume of activation of the H_2O exchange reaction is defined as follows:

$$\Delta V^* = -RT \left(\frac{\delta \ln k}{\delta P} \right)_T \quad (18)$$

The pressure dependence of the exchange rate is usually expressed as a quadratic function [23], that is:

$$\ln k_p = \ln k_0 - \frac{\Delta V_0^* \cdot P}{RT} + \frac{\Delta \beta^* \cdot P^2}{2RT} \quad (19)$$

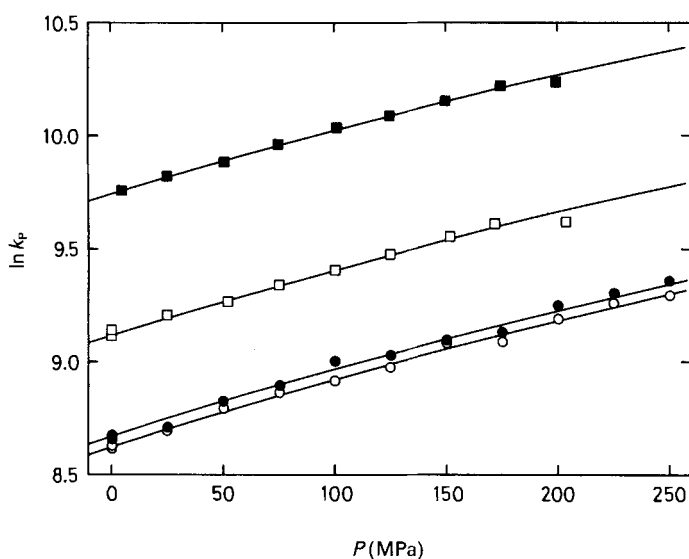
where k_0 is the rate constant at zero pressure, ΔV_0^* is the volume of activation at zero pressure and $\Delta \beta^*$ is the compressibility coefficient of activation.

Four variable pressure experiments were run, two at 1.4 T with sample 3 at 336.1 K and with sample 6 at 337.7 K, and two at 4.67 T with sample 7 at 345.1 K and 358.1 K (Table 5). The temperature range of these experiments was chosen so that the main contribution to the bulk H_2O line-width comes from $1/\tau_m$. The H_2O exchange rates at each pressure, k_p , have been calculated from the experimental $1/T_{2r}$ using Eqn. 14, in which the parameters of $1/T_{2os}$ and $\Delta \omega_m$ were fixed to the values found in the variable-temperature study. Then the calculated k_p 's were fitted with Eqn. 19, the adjustable parameters being k_0 , ΔV_0^* and $\Delta \beta^*$. The four sets of data gave remarkably similar values of ΔV_0^* , all within $0.4 \text{ cm}^3 \text{ mol}^{-1}$, but without significant trend with temperature. Thus an overall fit of the

Table 5. Relaxation Rates, $1/T_2$, of the Bulk H_2O in Presence of $V(CF_3SO_3)_3$ as a Function of Pressure (for the composition of the solutions, see Table 1)

Solution 3 336.1 K		Solution 6 337.7 K		Solution 7 345.1 K		Solution 7 358.1 K	
P [MPa]	$1/T_2^a)$ [s ⁻¹]	P [MPa]	$1/T_2^a)$ [s ⁻¹]	P [MPa]	$1/T_2^b)$ [s ⁻¹]	P [MPa]	$1/T_2^b)$ [s ⁻¹]
0.1	1094	0.1	1049	0.1	379.5	5.0	636.6
50.3	1265	50.0	1198	52.1	427.9	50.7	714.0
100.0	1412	100.0	1405	100.1	480.3	101.5	818.9
150.0	1647	150.2	1526	152.1	545.4	150.0	912.3
200.3	1812	200.0	1755	204.0	575.6	199.5	986.1
249.9	1988	249.8	1938	175.0	571.8	174.7	971.9
225.0	1928	225.2	1844	125.0	510.3	125.0	859.2
175.0	1648	175.0	1576	75.0	455.7	75.0	765.3
125.0	1487	125.1	1437	25.0	408.3	25.1	672.8
75.0	1348	75.2	1271	0.1	386.6		
25.4	1164	25.1	1079				
0.1	1085	0.1	1032				

a) At 8.133 MHz. b) At 27.11 MHz.


 Fig. 5. Water exchange rates on $V(H_2O)_6^{3+}$ as a function of pressure. \circ : soln. 3, at 336.1 K and 1.4 T; \bullet : soln. 6, at 337.7 K and 1.4 T; \square : soln. 7, at 345.1 K and 4.67 T; \blacksquare : soln. 7, at 358.1 K and 4.67 T.

data was carried out with six adjustable parameters, that is ΔV_0^* , $\Delta\beta^*$ and four k_0 's. Fig. 5 shows the calculated k_p values and the fitted curves; the adjusted activation parameter values are $\Delta V_0^* = -8.86 \pm 0.38 \text{ cm}^3 \text{ mol}^{-1}$ and $\Delta\beta^* = -(1.06 \pm 0.32) \cdot 10^{-2} \text{ cm}^3 \text{ mol}^{-1} \text{ MPa}^{-1}$.

Discussion. – In [8] using acidified VCl_3 solutions we observed at 298 K two bound ^{17}O signals besides that of the hexaaqua ion, one at + 307 ppm and one, badly resolved, at – 69 ppm from $V(H_2O)_6^{3+}$ (the free H_2O signal lies at about + 2600 ppm). The integration

of these two signals, tentatively assigned to axial and equatorial H_2O molecules of $\text{V}(\text{H}_2\text{O})_5\text{Cl}^{2+}$, indicated a percentage of 5–10% of monochloro complex in a 1.5 *m* VCl_3 and 2.0 *m* HCl solution; at 352 K, this percentage reaches nearly 50%. Because of the lower coordinating ability of the bromide, the proportion of monobromo complex in VBr_3 solutions is smaller, but not negligible. The presence of halocomplexes is also demonstrated by ^{35}Cl -, ^{37}Cl -, ^{79}Br - and ^{81}Br -NMR. The environment of the coordinated halide is too unsymmetrical to give rise to an observable signal, but the variation of the line-width of the free halide signal with increasing temperature is informative: it first narrows as expected for a quadrupolar relaxation mechanism, reaches a minimum at 310 K for the chloride and 370 K for the bromide, and finally broadens rapidly, due to chemical exchange between the free and coordinated sites. This interpretation is confirmed by the fact that, for each halide, the line-widths of both isotopes are in the same ratio as the squares of their quadrupole moments at low temperature, while they are equal at high temperature (since the exchange broadening is independent of the nuclear properties of the isotopes).

In the present work, we chose CF_3SO_3^- as counter-ion to avoid the problem of complexation. The ^{17}O -NMR spectra of a vanadium triflate solution (*Fig. 3*) show only one coordinated H_2O signal, and a variable-temperature ^{19}F -NMR study of this solution revealed no exchange broadening of the ^{19}F signal, even at high temperature. Thus, we are confident that no complexation of the V^{3+} ion occurs when triflate is the counter-ion.

The presence of halo complexes could be a reason for the differences between the kinetic parameters obtained by *Chmelnick* and *Fiat* [7], using Cl^- and Br^- as counter-ions, and ours (see *Table 6*). A further reason for these differences is that the ^{17}O transverse relaxation rates were measured in a smaller temperature range in the former study. Only the slow exchange domain was covered, and the experimental data were consequently analyzed with the simplified equation $1/T_{2r} = 1/\tau_m$. It was clearly demonstrated by *Newman et al.* [17] that such simplified equations are inadequate for the determination of activation parameters.

Table 6. Kinetic Parameters for H_2O Exchange on $\text{V}(\text{H}_2\text{O})_5^{2+}$

	<i>Chmelnick</i> and <i>Fiat</i> [7]	This study
$10^{-2} \cdot k^{298}$ [s^{-1}]	16.7	5.0 ± 0.3
ΔH^* [kJ mol^{-1}]	25.9	49.4 ± 0.8
ΔS^* [$\text{JK}^{-1} \text{mol}^{-1}$]	-96	-27.8 ± 2.2
ΔV^\ddagger [$\text{cm}^3 \text{mol}^{-1}$]	-	-8.9 ± 0.4
$10^2 \cdot \Delta\beta^*$ [$\text{cm}^3 \text{mol}^{-1} \text{MPa}^{-1}$]	-	-1.1 ± 0.3

The negative value of ΔS^* , we found, is consistent with an associative activation mode. However, the activation entropy as determined in NMR studies of solvent exchange on paramagnetic metal ions is not always a conclusive criterion for the assignment of the activation mode: *i*) it is obtained by a long extrapolation of $\ln(k/T)$ values to $1/T = 0$, and *ii*) the rate constants may be subject to systematic errors when other relaxation mechanisms present also an important contribution to the observed line-width [17]. The volume of activation is a more reliable parameter from that point of view, since it is proportional to the slope of the $\ln k$ vs. pressure curve. Furthermore, a change of volume is easier to visualize and interpret than a change of entropy ('disorder'), particularly in a symmetrical reaction.

The negative value found for the activation volume of the H₂O exchange reaction on V(H₂O)₆³⁺ indicates unambiguously that the activation mode of this reaction is associative. Moreover, the fitted value of Δβ*, the compressibility coefficient of activation, is negative and significantly different from zero, as is apparent from the slight curvature of the experimental data with pressure on Fig. 5; this value is comparable to the value proposed by Stranks for an associative A mechanism (−7.2 · 10^{−3} cm³ mol^{−1} MPa^{−1} [24]). The experimental data are not precise enough to authorize a quantitative discussion on the magnitude of this second-order parameter, but it indicates that the exchange mechanism is close to a limiting A mechanism. We are more inclined to propose an associative interchange mechanism I_a, however, because our fitted volume of activation is still more positive than that calculated for a limiting associative mechanism (−13.5 cm³ mol^{−1}), according to Swaddle's semi-empirical model [25].

For divalent high-spin hexasolvated transition metal ions, a trend in the volumes of activation for H₂O exchange reactions was observed along the series: the early members show I_a behaviour, and the later ones I_d behaviour. This gradual changeover can be explained by the variation of the radius of the metallic ions and by the filling of the d orbitals along the series [2]. By analogy, the volume of activation for the H₂O exchange reaction for trivalent ions is thus expected to increase from the d² V³⁺ ion (−8.9 cm³ mol^{−1}) to the d³ Cr³⁺ ion (−9.6 cm³ mol^{−1} [5]) then to the d⁵ Fe³⁺ ion (−5.4 cm³ mol^{−1} [6]). One must not be worried by the slightly less negative value found for V(H₂O)₆³⁺ as compared to that of Cr(H₂O)₆³⁺: it is generally accepted that the determination of ΔV* is subject to an experimental uncertainty of ±1 cm³ mol^{−1}, either with the isotopic dilution technique used

Table 7. Rate Constants for Complex-Formation Reactions with V(H₂O)₆²⁺ at 298 K

Ligand	pK _a ^{a)}	k _f [M ^{−1} s ^{−1}]	Reference
Cl [−]		≤ 3	[28]
Br [−]		≤ 10	[28]
NO ₂ H ₂ Sal ^b		3.5	[27]
H ₂ Sal ^c		4.9	[29]
⁺ NH ₃ H ₂ Sal		3.3	[26]
NH ₂ H ₂ Sal ^d		3.3 to 25 ^e	[26]
HN ₃		(0.4) ^f	[30]
NCS [−]	−1.84	114, 104	[31] [32]
H ₂ O	−1.74	54	This work
HOOC−COO [−]	1.20	1.3 · 10 ³	[28]
NO ₂ HSal [−]	2.24	1.23 · 10 ³	[27]
HSal [−]	2.80	1.4 · 10 ³	[29]
HOOC−CH ₂ −COO [−]	2.83	3.8 · 10 ³	[33]
⁺ NH ₃ HSal [−]	2.84 to 3.44	(1.6 to 7.0) · 10 ^{3e}	[26]
NH ₂ HSal [−]	3.60	7 · 10 ³	[26]
N ₃ [−]	4.15	(9 · 10 ²) ^f	[30]

a) Dissociation constants of the acids conjugate to the active sites of the ligands.

b) 5-Nitrosalicylic acid.

c) Salicylic acid.

d) 4-Aminosalicylic acid.

e) No precise value available, due to mechanistic ambiguities (see [26] for details on the estimation of the limits).

f) Calculated from the rate constant of the back reaction and an equilibrium constant which is low and, therefore, not accurately measurable.

for Cr^{3+} or with the NMR technique used for all other hexaquaions. It may also be pointed out that V^{3+} and Fe^{3+} ions have the same radius, 64 pm [20]; the less associative character of the latter ion can thus be exclusively attributed to electronic effects: stronger repulsion towards the incoming ligand due to higher t_{2g} orbitals occupancy, and easier bond breaking with the leaving ligand when the e_g^* anti-bonding orbitals are half-filled.

Our observation that the acidity of our solutions did not affect the results is corroborated by the remarks of some authors of complex formation kinetic studies on $\text{V}(\text{H}_2\text{O})_6^{3+}$ (see e.g. [26–29] and [31–32] in Table 7): contrary to what happens with other trivalent metal ions, these authors noted that the hydrolyzed species $\text{V}(\text{H}_2\text{O})_5\text{OH}^{2+}$ is less reactive than the hexaquo species. However, as pointed out by *Perlmutter-Hayman* and *Tapuhi* [27], the lack of reactivity of the hydrolyzed species is not a proof of an associative activation mode for substitution reactions on V^{3+} . The arguments in favour of such an activation mode for substitution on this ion lay on the comparison of the complex formation rate constants, k_f . The available results are listed in Table 7 in the order of increasing basicity of the active site of the ligands, as it was already done by *Perlmutter-Hayman* and *Tapuhi* [26], rather than classified with respect to their electrostatic charge.

According to the *Eigen-Wilkins* model, these rate constants could be decomposed as the product of two terms, the outer-sphere association constant, K_{os} , and the rate constant for the interchange within the encounter complex, k_i ; then the H_2O exchange rate, k_{ex} , should be compared to the k_f 's for the discussion on the activation mode. However, K_{os} cannot be measured with the techniques used in the above studies, and even its calculation by *Fuoss*' theoretical model would be questionable for large ligands like salicylates. The *Eigen-Wilkins* model is indeed valuable for dissociatively activated substitutions, where the rate-determining step is the departure of a molecule of H_2O , so $k_i \approx k_{ex}$. But for associatively activated reactions, k_i is in any case dependent on the nature of the incoming ligand, and it appears of better value to compare the experimental k_f values than to divide them by a dubious K_{os} factor and to consider the intrinsically different k_f 's. To compare the water exchange rate with the complex-formation rate constants, one must first multiply k_{ex} by the factor 6/55.5, to obtain a second-order rate constant.

The correlation between the rate constants and the basicities of the incoming ligands is obvious (Table 7); if the slower rate observed for H_2O as compared to the less basic thiocyanate may be explained by a charge effect, the difference in the rates of 5-nitrosalicylic acid and 5-nitrosalicylate, for instance, is too large to be ascribed solely to such effect. The strong dependence of k_f upon the nature of the incoming ligand can, therefore, be presented as evidence for the associative activation mode of substitution reactions on $\text{V}(\text{H}_2\text{O})_6^{3+}$. This interpretation is now confirmed by the negative volume of activation for the water exchange reaction, and we can ascribe an I_a mechanism to these reactions.

We thank the *Swiss National Science Foundation* for financial support (grant No. 2.024-0.83).

REFERENCES

- [1] L. Helm, L. I. Elding, A. E. Merbach, *Helv. Chim. Acta* **1984**, *67*, 1453.
[2] A. E. Merbach, *Pure Appl. Chem.* **1982**, *54*, 1479.
[3] F. K. Meyer, K. E. Newman, A. E. Merbach, *J. Am. Chem. Soc.* **1979**, *101*, 5588; Y. Ducommun, K. E. Newman, A. E. Merbach, *Inorg. Chem.* **1980**, *19*, 3696.
[4] D. R. Stranks, T. W. Swaddle, *J. Am. Chem. Soc.* **1971**, *93*, 2783.
[5] San-chou Xu, H. R. Krouse, T. W. Swaddle, *Inorg. Chem.* **1985**, *24*, 267.
[6] T. W. Swaddle, A. E. Merbach, *Inorg. Chem.* **1981**, *20*, 4212.
[7] A. M. Chmelnick, D. Fiat, *J. Magn. Reson.* **1972**, *8*, 325.
[8] Y. Ducommun, L. Helm, A. Hugi, D. Zbinden, A. E. Merbach, Proceedings of the Joint Meeting of the 8th AIRAPT and 19th EHPRG Conferences-Uppsala (1981), in 'High Pressure in Research and Industry', Eds. C. M. Backman, T. Johannisson, and L. Tegnér, Uppsala, 1982, Vol. 2, pp. 684–687.
[9] M. L. Martin, J.-J. Delpuech, G. J. Martin, 'Practical NMR Spectroscopy', Heyden & Son, Ltd, London, 1980, p. 163.
[10] A. Monnerat, Ph. D. Thesis, University of Lausanne, 1981.
[11] D. L. Pisanelli, L. Helm, P. Meier, A. E. Merbach, *J. Am. Chem. Soc.* **1983**, *105*, 4528.
[12] C. Ammann, P. Meier, A. E. Merbach, *J. Magn. Reson.* **1982**, *46*, 319.
[13] A. Monnerat, P. Moore, K. E. Newman, A. E. Merbach, *Inorg. Chim. Acta* **1981**, *47*, 139.
[14] T. J. Swift, R. E. Connick, *J. Chem. Phys.* **1962**, *37*, 307; *ibid.* **1964**, *41*, 2553.
[15] J. Burgess, 'Metal Ions in Solution', Ellis Horwood, Ltd, Chichester, 1978, p. 148.
[16] N. Bloembergen, *J. Chem. Phys.* **1957**, *27*, 595.
[17] K. E. Newman, F. K. Meyer, A. E. Merbach, *J. Am. Chem. Soc.* **1979**, *101*, 1470.
[18] J.-P. Kintzinger, in 'NMR Basic Principles and Progress', Eds. P. Diehl, E. Fluck and R. Kosfeld, Springer-Verlag, Berlin, 1981, Vol. 17, pp. 39–45.
[19] H. G. Hertz, in 'Progress in NMR Spectroscopy', Eds J. W. Emsley, J. Feeney and L. H. Sutcliffe, Pergamon Press, Oxford, 1967, Vol. 3, p. 191.
[20] R. D. Shannon, *Acta Crystallogr., Sect. A* **1976**, *32*, 751.
[21] B. Halle, H. Wennerström, *J. Chem. Phys.* **1981**, *75*, 1928.
[22] D. Hugi-Cleary, L. Helm, A. E. Merbach, to be published.
[23] H. Kelm, D. A. Palmer, in 'High Pressure Chemistry', NATO Advanced Study Institutes Series: Series C, Ed. H. Kelm, D. Reidel Publishing Company, Dordrecht, 1978, Vol. 41, pp. 281–309.
[24] D. R. Stranks, *Pure Appl. Chem.* **1974**, *38*, 303.
[25] T. W. Swaddle, *Inorg. Chem.* **1983**, *22*, 2663.
[26] B. Perlmutter-Hayman, E. Tapuhi, *Inorg. Chem.* **1979**, *18*, 2872.
[27] B. Perlmutter-Hayman, E. Tapuhi, *J. Coord. Chem.* **1980**, *10*, 219.
[28] R. C. Patel, H. Diebler, *Ber. Bunsenges. Phys. Chem.* **1972**, *76*, 1035.
[29] B. Perlmutter-Hayman, E. Tapuhi, *J. Coord. Chem.* **1979**, *9*, 177.
[30] J. H. Espenson, J. R. Pladziewicz, *Inorg. Chem.* **1970**, *9*, 1380.
[31] B. R. Baker, N. Sutin, T. J. Welch, *Inorg. Chem.* **1967**, *6*, 1948.
[32] W. Kruse, D. Thusius, *Inorg. Chem.* **1968**, *7*, 464.
[33] P. N. Mathur, H. Fukutomi, *J. Inorg. Nucl. Chem.* **1981**, *43*, 2869.